Available online at BCREC website: https://bcrec.id

Bulletin of Chemical Reaction Engineering & Catalysis, 17 (1) 2022, 1-12

Research Article

Catalytic Decomposition of Methane to Hydrogen over Al_2O_3 Supported Mono– and Bimetallic Catalysts

Gaukhar Yergaziyeva[1,2,*], Nursaya Makayeva[2], Zhanna Shaimerden[2], Sergiy Soloviev[3], Moldir Telbayeva[1], Erzhan Akkazin[2], Fariza Ahmetova[2]

[1]Institute of Combustion Problems, Bogenbay batyra, 172 A, 050012 Almaty, Kazakhstan.
[2]Al-Farabi Kazakh National University, al- Farabi ave. 71, 050040 Almaty, Kazakhstan.
[3]L.V. Pysarzhevskii Institute of Physical Chemistry, National Academy of Sciences of Ukraine, Prospekt Nauki, 31, 03028 Ukraine.

Received: 27th August 2021; Revised: 5th October 2021; Accepted: 7th October 2021
Available online: 14th October 2021; Published regularly: March 2022

Abstract

This article discusses the decomposition of methane in the temperature range 550–800 °C on low-percentage monometallic (Ni/γ-Al_2O_3, Co/γ-Al_2O_3) and bimetallic (Ni-Co/γ-Al_2O_3) catalysts. It is shown that the bimetallic catalyst is more active in the decomposition of methane to hydrogen than monometallic ones. At a reaction temperature of 600 °C, the highest methane conversion is 81%, and the highest hydrogen yield of 51% is formed on Ni-Co/γ-Al_2O_3. A complex of physicochemical methods (Scanning Electron Microscope (SEM), X-ray Diffraction (XRD), Temperature Programmed Reduction (TPR-H_2), *etc.*) established that the addition of cobalt oxide to the composition of Ni/γ-Al_2O_3 leads to the formation of surface bimetallic Ni-Co alloys, while the dispersion of particles increases and the reducibility of the catalyst is facilitated, which provides an increase in the concentration of metal particles - active centers, which can be the reason for an increase in the catalytic properties of a bimetallic catalyst in comparison with monometallic ones.

Copyright © 2021 by Authors, Published by BCREC Group. This is an open access article under the CC BY-SA License (https://creativecommons.org/licenses/by-sa/4.0).

Keywords: methane decomposition; Al_2O_3 catalyst; hydrogen; bimetallic catalyst; Ni/γ-Al_2O_3; Co/γ-Al_2O_3; Ni-Co/γ-Al_2O_3

How to Cite: G. Yergaziyeva, N. Makayeva, Z. Shaimerden, S. Soloviev, M. Telbayeva, E. Akkazin, F. Ahmetova (2022). Catalytic Decomposition of Methane to Hydrogen over Al_2O_3 Supported Mono- and Bimetallic Catalysts. *Bulletin of Chemical Reaction Engineering & Catalysis*, 17(1), 1-12 (doi:10.9767/bcrec.17.1.12174.1-12)

Permalink/DOI: https://doi.org/10.9767/bcrec.17.1.12174.1-12

1. Introduction

In connection with the transition to "green" technology, intensive work is underway throughout the world to find alternative energy sources and energy carriers. One of the most promising modern energy carriers is hydrogen, which is determined by its ecological purity, versatility and high efficiency of energy conversion processes with its participation [1]. Currently, the most common technologies for the production of hydrogen are: steam reforming of methane (SRM) [2,3], catalytic decomposition of methane (CDM) [4,5], partial oxidation of methane (POM) [6,7], gasification of coal and other hydrocarbons [8], water electrolysis [9,10], photocatalytic water splitting [11,12], biomass gasification [13]. Compared to fossil fuels, other hydrocarbons and biomass, methane is the best source for hydrogen production because it is easy to mine and has a high hydrogen to carbon

* Corresponding Author.
Email: ergazieva_g@mail.ru (G. Yergaziyeva);
Telp.: +77073143584

ratio [14–16]. Commercial hydrogen is produced using a SRM. The advantages of the CDM are that the specific CO_2 emissions for hydrogen production are significantly lower compared to the CDM. In addition, the production of nanocarbon as a by-product in CDM will make this process economically competitive compared to SRM [17–19]. The production of hydrogen from natural gas, the main component of which is methane, is of great practical importance as the world's known reserves of natural gas are increasing [20]. Compared to electrolysis of water, the main advantage of CDM is the ease of use of raw materials and their availability [18]. Photocatalytic water splitting into hydrogen and oxygen with zero greenhouse gas emissions using photoelectrodes is very valuable for the energy [21,22]. However, photoelectrode materials that have special catalytic characteristics and stability in a light environment have not yet been found [23].

Due to the aforementioned advantages in the latter, CDM to hydrogen and nanocarbon attracts the attention of scientists [24]. The most commonly used catalysts in SRM are transition metals, including Ni, Co, and Fe, on supports including Al_2O_3, SiO_2, TiO_2, MgO, CeO_2, carbon, and zeolites [25–27]. Iron-based catalysts are more stable to carbonization, but have low activity in the decomposition of methane [28]. Carbon-based catalysts give lower methane conversion than metal catalysts [29]. Among these catalysts, supported nickel catalysts have been extensively studied for their favorable activity under pyrolysis operating conditions. Nickel-based catalysts are highly active in CDM, but they are sensitive to operating temperature and quickly deactivated at high temperatures [30]. The content of nickel oxide on the support varies from 0.5–60 wt% [31]. It is assumed that catalysts with a nickel oxide content in the range of 0.5–5 wt% are less susceptible to carbonization [32]. The addition of modifying additives (noble metals, oxides of cobalt, cerium, *etc.*) to nickel-based catalysts can improve the activity and stability of the catalyst in the decomposition of methane [33]. The novelty of this work is a study of the decomposition of methane on catalysts with a low content of nickel oxide on a support, a comparison of the activity of low-percentage monometallic ($Ni/\gamma\text{-}Al_2O_3$, $Co/\gamma\text{-}Al_2O_3$) and bimetallic ($Ni\text{-}Co/\gamma\text{-}Al_2O_3$) catalysts in this process.

This work aims is a comparative study of the activity in the decomposition of methane and physicochemical characteristics of low-percentage monometallic and bimetallic nickel, cobalt-containing catalysts. The catalysts were synthesized by capillary impregnation of the support to incipient wetness with solutions of nitric acid salts of the metals. The catalysts have been tested in the decomposition of methane. The physicochemical characteristics of the catalysts were studied by N_2 physisorption, TPR-H_2, SEM, XRD, and TGA. The method of synthesis is an effective one for concentrating the active phase on the surface of the support, which is very important in the synthesis of low-percentage catalysts. Active centers are more accessible for reactant molecules. The method utilizes several advantages, *e.g.* relative simplicity, less hazardous waste, and more efficient use of a low-percentage active component, there is no loss of impregnating solution, which is especially important in the manufacture of expensive catalysts [34,35].

2. Materials and Methods

2.1 Preparation of catalysts

Monometallic catalysts $x\text{Ni}/\gamma\text{-}Al_2O_3$ and $y\text{Co}/\gamma\text{-}Al_2O_3$ (where x is the content of oxides in the catalyst, wt%) were obtained by capillary impregnation of $\gamma\text{-}Al_2O_3$ support (S_{BET}=180 m^2/g, Changhai Jiuzhou Chemicals Co) with aqueous solutions of $Ni(NO_3)_2.6H_2O$ (technical standard 4055-70) or $Co(NO_3)_2.6H_2O$ (technical standard 4528-78). The content of oxides in the catalyst is 3 wt%.

Bimetallic $x\text{Ni}\text{-}y\text{Co}/\gamma\text{-}Al_2O_3$ (where x and y are the content of metal oxides in the catalyst, wt %) catalysts were also prepared by capillary impregnation of $\gamma\text{-}Al_2O_3$ support (S_{BET}=180 m^2/g, Changhai Jiuzhou Chemicals Co) with aqueous solutions of a mixture of salts metals $Ni(NO_3)_2.6H_2O$ (technical standard 4055-70) или $Co(NO_3)_2.6H_2O$ (technical standard 4528-78). The ratio of oxides in the bimetallic sample was Ni:Co (1:2). Heat treatment of all samples was carried out in air at 300 °C for 2h, then at 500 °C for 3 h.

2.2 Characterization of Catalysts

The physicochemical characteristics of the catalysts were studied by X-ray diffraction (XRD), N_2 physisorption, scanning electron microscopy (SEM), temperature-programmed hydrogen reduction (TPR-H_2), and thermogravimetric analysis (TGA).

2.2.1 N_2 Physisorption

Determination of the textural properties of the developed catalysts and carriers (specific surface area (SSA), pore volume and pore size

Copyright © 2021, ISSN 1978-2993

distribution) was carried out by the method of low-temperature adsorption of nitrogen at 77 K on an automatic installation BEL Japan Inc. and thermal desorption of argon using a BEL-SORP-mini II device. Before testing the sample, its degassing is carried out, which consists in heating the sample in a stationary gas flow at a given temperature in order to remove the gases and vapors absorbed by it from the surface of the test material. Pressure sensor is 0.666 Pa/min. The mass of the catalyst loading is 2.92 g, the run time is 3 hours, saturated steam pressure 102.19 kPa, and V_m = 30.563 $cm^3(STP).g^{-1}$. The surface area is calculated using the BET (Brunauer–Emmett–Teller) equation.

2.2.2 Scanning Electron Microscopy (SEM)

Scanning electron microscopy was carried out on a JEOL JSM-6390 LA device with a JED 2300 energy-dispersive X-ray detector. Surface micrographs were obtained in the modes of registration of secondary electrons (topographic contrast) and backscattered electrons (contrast depending on the atomic number). The elemental composition of the surface of the samples was determined using a JED 2300 energy-dispersive X-ray detector (resolution 133 eV). The calculation of the percentage of each element in the analyte was carried out from the obtained X-ray spectra using the Analysis Station software version 3.62.07. (JEOL Engineering) using the standard-free ZAF method.

2.2.3 Temperature-programmed reduction of hydrogen (TPR-H_2)

Temperature-programmed reduction with hydrogen (TPR-H_2) was carried out on a USGA-101 unit (Russia), which included a gas treatment system, a flow-through reactor (inner diameter 4 mm) with a tube furnace, and a thermal conductivity detector. The sample (100 mg, fraction 0.30–0.50 mm) was preliminarily purged with Ar at 480 °C for 40 min, followed by cooling to 50 °C, and then heated at a rate of 10 °C/min from 50 to 950 °C in a mixture flow of 10 vol% H_2 in Ar at a feed rate of 30 cm^3/min. The analysis of the gas mixture was carried out using a thermal conductivity detector.

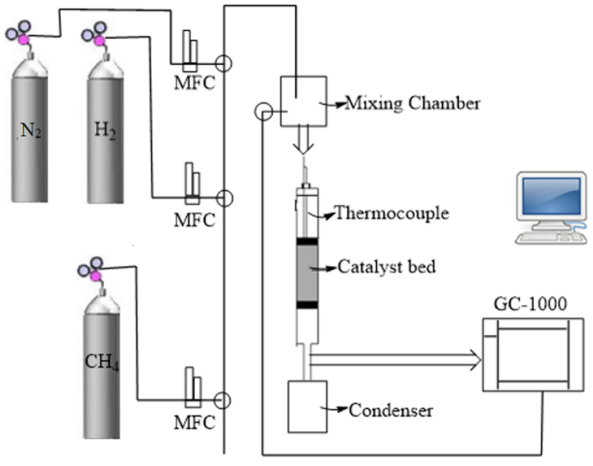

Figure 1. Scheme of an flow-through installation.

2.2.4 Thermogravimetric Analysis (TGA)

The analyzes were carried out on a derivatograph of the "MOM" company - Budapest (Hungary). The method used is based on the device registering changes in the thermochemical and physical parameters of a substance, which can be caused by heating it. The analysis was carried out in air, in the temperature range from 20 to 1000 °C. The furnace heating mode is linear (dT/dt = 10), the reference substance is calcined Al_2O_3. For unambiguity, shooting conditions, the weighed amount of samples No 1, 2, 3 and 4 was strictly 200 mg, with a sensitivity of the scales - 50 mg. The analysis was filmed within the following measuring systems of the device: DTA = 250 μV, DTG = 500 μV, TG = 500 μV, T = 500 μV. Samples for analysis were filled into platinum micro crucibles.

2.2.5 X-ray diffraction (XRD)

X-ray diffraction measurements were made using a Bruker D8 ADVANCE A25 powder X-ray diffractometer (Cu-Kα radiation (λ = 1.5406 Å), Ni-filter on secondary radiation) at room temperature by the polycrystal method. To obtain representative X-ray diffraction patterns, the survey was carried out at long accumulation times (2 s), a scanning step of 0.02° in 2θ in the range of angles 10–90°.

2.3 Testing the activity of catalysts

The decomposition of methane was carried out on a flow-through laboratory setup (Figure 1). The catalysts were placed in a quartz reactor (length 36 cm, inner diameter 1.7 cm). The volume of the catalyst in the reactor is 2 ml. The shape of the catalysts is granules with a diameter of 2–3 mm.

Process conditions: pressure P = 0.1 MPa, reaction temperature T_r = 500–800 °C, ethanol volumetric flow rate WHSV = 4980 h^{-1}. Before the reaction, the catalysts were reduced with

Copyright © 2021, ISSN 1978-2993

hydrogen at 600 °C for 3 hours. After the reduction of the catalysts, hydrogen was removed by a stream of nitrogen from the reaction system, then a methane/nitrogen mixture was fed at a given temperature with a flow rate of 160 ml/min, the methane content in the initial reaction mixture was 6 vol%.

2.4 Analysis of Reaction Products

The reaction products were identified by gas chromatography using a "Chromos GH-1000 chromatograph" (Russia). For the analysis of hydrogen, a packed column (l = 1 m, d = 2 mm) containing the CaA adsorbent was used. The column temperature was increased from 50 to 240 °C (rate of change 20 °C/min). The injector and detector temperatures were 200 °C and 250 °C, respectively. The following gas flow rates were used: argon 20 mL/min, hydrogen 20 mL/min, air 200 mL/min. An HP/PlotQ column was used to identify CH_4, CO_2, and CO.

The efficiency of the catalysts was expressed in terms of methane conversion. The first analysis was carried out about 15 minutes after the methane was passed over the catalyst. Methane conversion and yield of hydrogen were calculated according to the Equations (1) and (2):

$$CH_4\ conversion\,(\%) = \frac{CH_{4,in} - CH_{4,out}}{CH_{4,in}} \times 100\% \qquad (1)$$

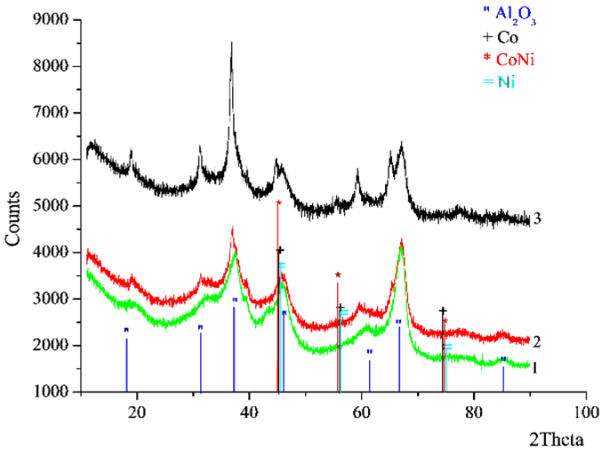

Figure 2. X-ray diffraction spectra of catalysts: 1) Co/γ-Al_2O_3; 2) Ni/γ-Al_2O_3; 3) Ni-Co/γ-Al_2O_3.

$$H_2\ yield\,(\%) = \frac{moles\ of\ hydrogen\ produced}{2 \times mole\ of\ CH_4\ in\ feed} \times 100\% \qquad (2)$$

where, the volume of CH_4 at the reactor inlet and outlet are represented by $CH_{4,in}$ and $CH_{4,out}$, accordingly.

3. Results and Discussion

3.1 Characterization of the Support and Supported Catalysts

The results of the texture characteristics of fresh samples are presented in Table 1. Table 1 shows that the pure γ-Al_2O_3 support has a developed surface (S_{sp} = 180.0 m^2/g) and specific pore volume 0.084 cm^3/g. The deposition of nickel or cobalt oxides leads to some increase in the characteristics of the support. Co-deposition of nickel and cobalt oxides increases the specific surface of the sample from 180.0 to 224.4 m^2/g, possibly due to the formation of a dispersed phase $NiCo_2O_4$. The formation of this phase is confirmed by the results of XRD (Figure 2) and TPR-hydrogen (Figure 2).

The X-ray diffraction patterns of the initial monometallic catalysts contain reflections of cobalt oxide (Co_3O_4), while the nickel oxide (NiO) phase cannot be detected, probably due to its high dispersion (less than 4 nm). The sample of the initial bimetallic Ni-Co/γ-Al_2O_3 catalyst contains a support phase (γ-Al_2O_3). The phase of cobalt oxide (Co_3O_4) is not fixed, as well as nickel oxide. The X-ray diffraction pattern of the catalyst sample also shows a metallic phase with a cubic face-centered lattice, the crystal cell parameter of this phase is 3.535–3.540 Å, judging by the value of the parameter, a Co-Ni solid solution with an fcc lattice is formed [36]. The size of the regions of coherent scattering of the metallic phase is ~23 nm. It is known [37] that the catalytic activity of oxide catalysts in redox reactions is explained by the oxygen-metal bond energy, the qualitative characteristics of which are the temperatures of the onset of the hydrogen reduction process, as well as the temperatures of the maxima on the TPR-H_2 curves.

The TPR-H_2 curves (Figure 3) for the Ni/γ-Al_2O_3 catalyst exhibit four peaks with maxima of hydrogen absorption temperatures T^1_{max} =

Table 1. Texture characteristics of samples.

Sample, content of oxides on the support, wt%	Specific surface, m^2/g	Specific pore volume, cm^3/g
γ-Al_2O_3	180.0	0.084
Ni/γ-Al_2O_3	212.6	0.098
Co/γ-Al_2O_3	210.6	0.090
Ni-Co/γ-Al_2O_3	224.4	0.096

Copyright © 2021, ISSN 1978-2993

458 °C, (Amount of hydrogen A = 5 μmol/gK$_t$), T^2_{max} = 545 °C, (A = 1 μmol/gKt), T^3_{max} = 655 °C, (A = 55 μmol/gK$_t$) and T^4_{max} = 814 °C, (A = 99 μmol/gK$_t$). According to the literature [38], the peak at T^1_{max} refers to the reduction of nickel cations in the composition of NiO particles not bound to the support. The peaks T^2_{max} T^3_{max} relate to the reduction of nickel oxide particles, which are characterized by "weak" and "strong" metal-carrier interactions [39,40]. An intense peak at T^4_{max} = 814 °C is due to the presence of dispersed spinel-like forms of $NiAl_2O_4$ in the sample [41]. The TPR profile of the Co/γ-Al_2O_3 sample is more complex than that of Ni/γ-Al_2O_3. The TPR-H_2 curves for Co/γ-Al_2O_3 catalyst show 5 peaks with maxima at T^1_{max} = 306 °C, (A = 3 μmol/gK$_t$), T^2_{max} = 424 °C, (A = 58 μmol/gK$_t$), T^3_{max} = 441 °C, (A = 58 μmol/gK$_t$), T^4_{max} = 639 °C, (A = 63 μmol/gK$_t$) and T^5_{max} = 796 °C, (A = 2 μmol/gK$_t$). The low-temperature peak at 306 °C is associated with the reduction of surface Co^{3+} to Co^{2+}, the second broad peak at higher temperatures (maxima at about 424, 441, and 639 °C), associated with the reduction of Co^{2+} species to metallic cobalt, depending on the interaction with the support [42]. The peak with a maximum at a temperature of about 796 °C corresponds to the reduction of a compound of the type of mixed oxides $CoAl_2O_4$ [43].

The bimetallic catalyst showed a complex reduction profile (Figure 3). A new peak appears at T^1_{max} = 205 °C (A = 80 μmol/gK$_t$), which was not previously observed for monometallic catalysts. According to the literature [44], the appearance of a new low-temperature peak is associated with the formation of a nickel-cobalt compound, $NiCo_2O_4$. The reduction of spinel $NiCo_2O_4$ was the subject of research by

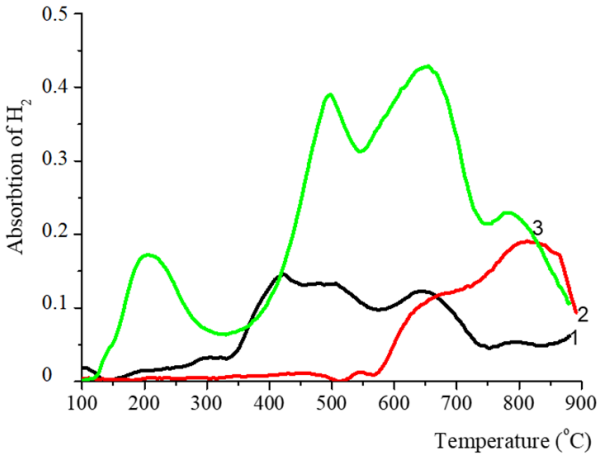

Figure 3. TPR-H_2 catalyst profiles: 1) Co/γ-Al_2O_3; 2) Ni/γ-Al_2O_3; 3) Ni-Co/γ-Al_2O_3.

Klissurski and Uzunova [45], who, analyzing the TPR of this compound in the temperature range 27-727 °C, observed three reduction peak, which were attributed to the gradual reduction of Ni^{2+}, Co^{3+}, and Co^{2+} cations statistically distributed in tetrahedral and octahedral spinel positions. The peaks with a maximum at temperatures of 315 °C and 367 °C, in the authors' opinion, correspond to the gradual reduction of $Co^{3+} \rightarrow Co^{2+}$ and $Co^{2+} \rightarrow Co^0$. The peak with a maximum at 257 °C is attributed to the reduction of Ni^{2+} cations.

Due to the possibility of several possible forms of the active phase in fresh cobalt-nickel catalysts, *i.e.* NiO, Co_3O_4, and $NiCo_2O_4$, it is difficult to unambiguously determine which peaks visible on the TPR profiles can be attributed to the reduction of a particular oxide form. Based on the available literature, we can only guess which peak corresponds to the recovery of a given phase.

In our case, a new low-temperature peak at T^1_{max} = 205 °C can be associated with the reduction of Ni^{2+} cations in the composition of $NiCo_2O_4$. It is believed [46] that the electronic conductivity of nickel-cobalt compounds is higher than that of the oxides NiO or Co_3O_4 themselves. An increase in the content of cobalt in the composition of the bimetallic catalyst led to a shift in the reduction temperature of their active phases towards higher temperatures (441, 458 → 497 °C). This phenomenon was observed in other works [47,48].

The peaks at T^2_{max} = 497 °C (A = 167 μmol/gK$_t$) and T^3_{max} = 655 ° C (A = 307 μmol/gK$_t$) can be associated with the overlapping of the reduction peaks of both nickel and cobalt. The increase in the amount of absorbed hydrogen can be associated with an increase in the content of cobalt oxide in the composition of the bimetallic catalyst (Ni-Co/γ-Al_2O_3) as compared to the monometallic catalyst Co/γ-Al_2O_3. The modification of nickel oxide with cobalt oxide leads to a decrease in the proportion of nickel in the composition of $NiAl_2O_4$, as evidenced by a decrease in the amount of absorbed hydrogen from 99 to 77 μmol/gK$_t$ and the reduction temperature from 814 to 779 °C in the bimetallic catalyst as compared to the monometallic sample Ni/γ-Al_2O_3. By reducing the proportion of nickel in the aluminate composition, part of the nickel is kept free on the catalyst surface, which can facilitate the formation of a nickel-cobalt compound during the reduction process. The formation of a nickel-cobalt compound is also confirmed by the results of XRD (Figure 2). According to the results of TPR-H_2 in the presence of a bimetallic

Copyright © 2021, ISSN 1978-2993

Ni-Co/γ-Al_2O_3 catalyst, a synergistic effect is observed due to the formation of the Ni_2CoO_4 alloy. In this case, the reducibility of the catalyst is facilitated, which ensures an increase in the concentration of metal particles - active centers.

The morphology of fresh catalysts was studied by scanning electron microscopy (Figure 4).

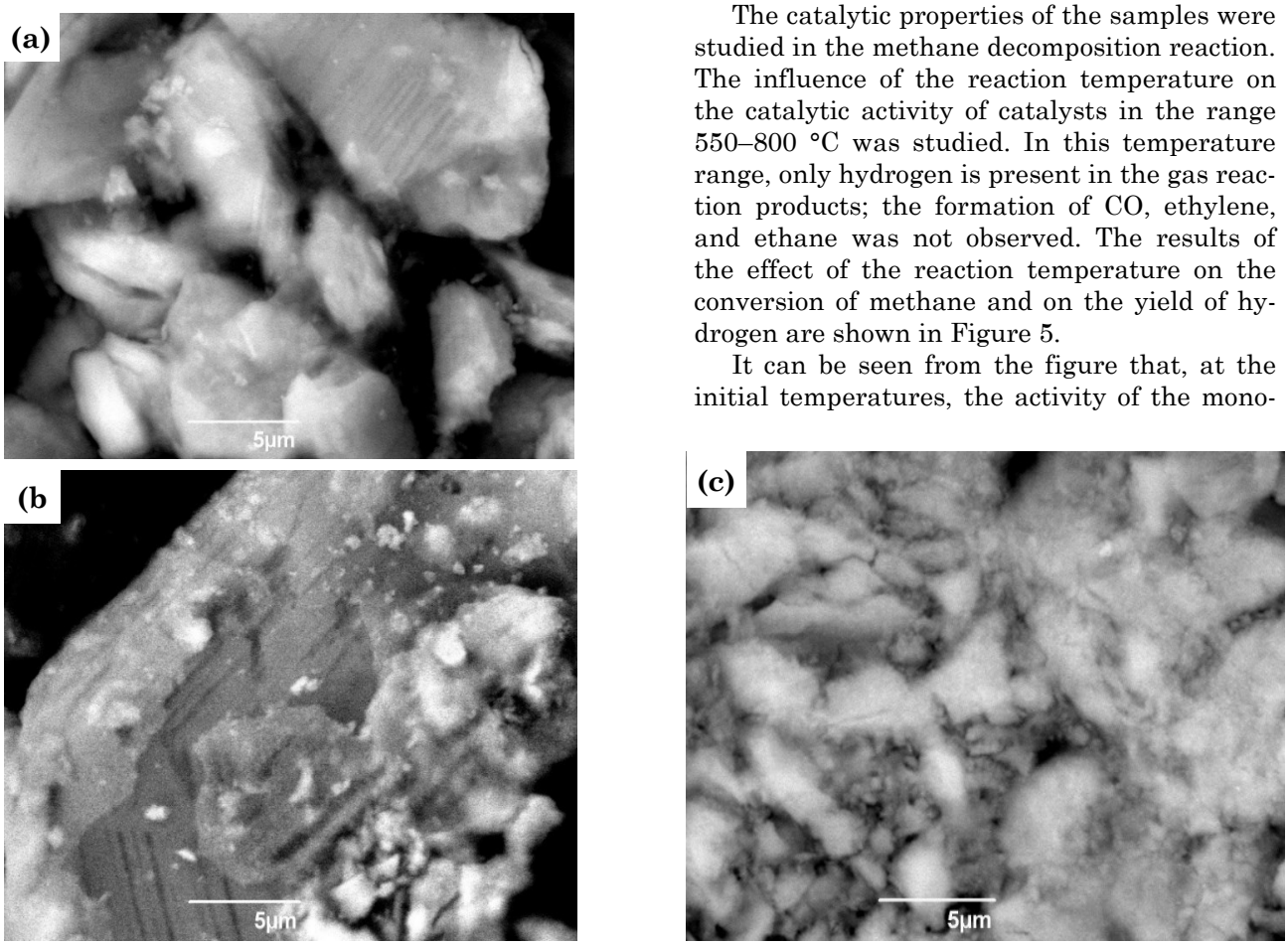

Figure 4. Micrographs of fresh catalysts; (a) Co/γ-Al_2O_3; (b) Ni/γ-Al_2O_3; (c) Ni-Co/γ-Al_2O_3.

The particle shapes of the monometallic samples have an irregular shape, nickel and cobalt oxides are not uniformly distributed on the surface of the support γ-Al_2O_3. It can be seen from the micrograph of the bimetallic catalyst that nickel and cobalt oxides are distributed more evenly and are located on the surface of Al_2O_3 granules mainly in the form of a uniform dispersion of nanosized particles.

The catalytic properties of the samples were studied in the methane decomposition reaction. The influence of the reaction temperature on the catalytic activity of catalysts in the range 550–800 °C was studied. In this temperature range, only hydrogen is present in the gas reaction products; the formation of CO, ethylene, and ethane was not observed. The results of the effect of the reaction temperature on the conversion of methane and on the yield of hydrogen are shown in Figure 5.

It can be seen from the figure that, at the initial temperatures, the activity of the mono-

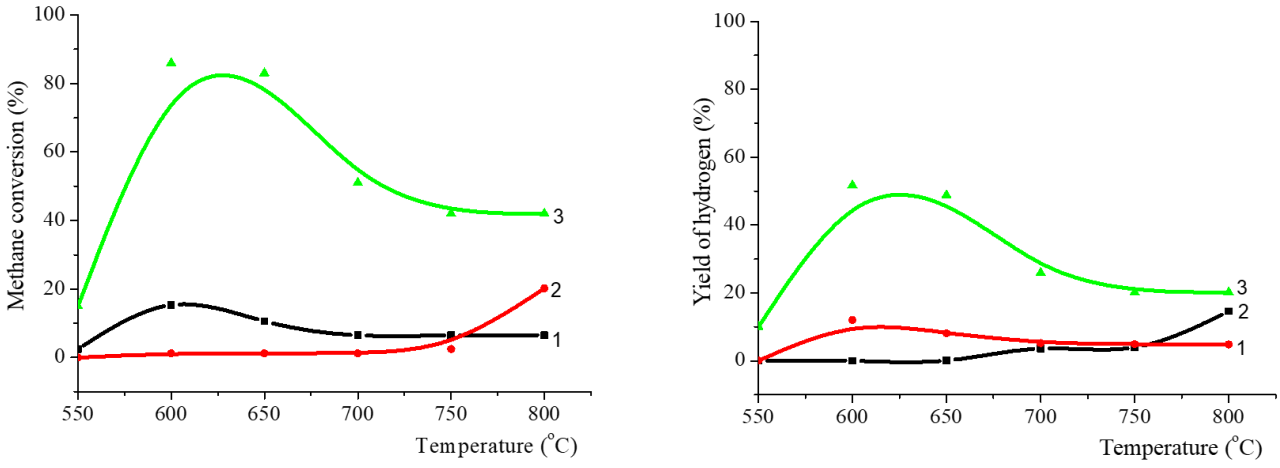

Figure 5. Influence of the reaction temperature on the conversion of methane and yield of hydrogen on catalysts: 1) Ni/γ-Al_2O_3; 2) Co/γ-Al_2O_3; 3) Ni-Co/γ-Al_2O_3.

Copyright © 2021, ISSN 1978-2993

metallic Ni/γ-Al_2O_3 catalyst is higher than that of Co/γ-Al_2O_3. With an increase in temperature, the activity of the nickel sample decreases, which is associated with the deactivation of nickel at high temperatures [49]. The Co/γ-Al_2O_3 has a low activity in the range 550–750 °C compared to Ni/γ-Al_2O_3. However, at a temperature of 800 °C, the conversion of methane reaches 20%, hydrogen is formed in the reaction products with a yield of 14.6%. Although Co/γ-Al_2O_3 as has a lower activity than the monometallic Ni catalyst, its addition helps to improve the activity of the bimetallic catalyst in the decomposition of methane.

The introduction of cobalt oxide into the Ni/γ-Al_2O_3 composition leads to an increase in the catalytic activity of the sample. The conversion of methane on the bimetallic Ni-Co/γ-Al_2O_3 catalyst in the studied temperature range is higher than on the monometallic one. The highest conversion of methane 86% is observed at a reaction temperature of 600 °C, hydrogen is formed in the gas products of the reaction with a yield of 51%.

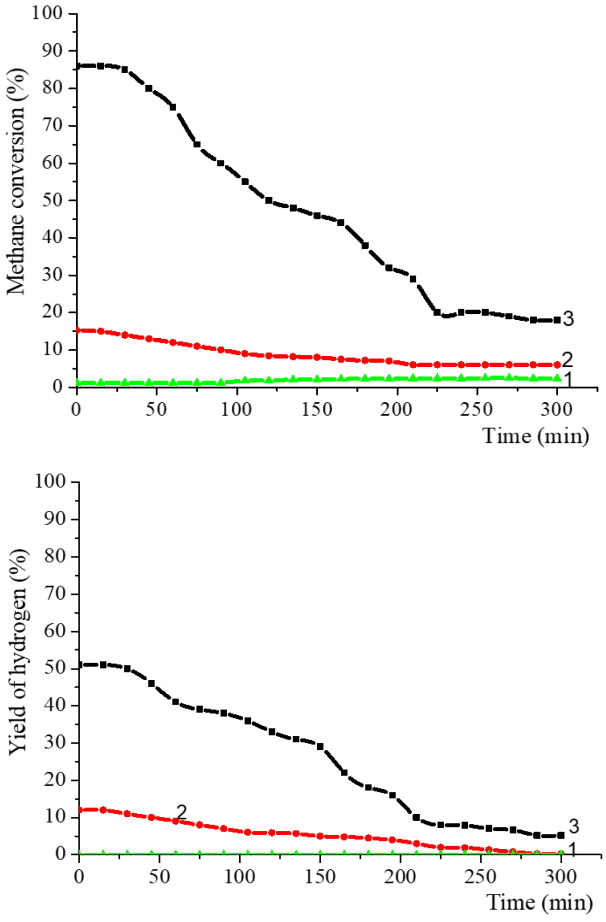

Figure 6. Influence of the reaction time on the conversion of methane and yield of hydrogen on catalysts at 600 °C: 1) Co/γ-Al_2O_3; 2) Ni/γ-Al_2O_3; 3) Ni-Co/γ-Al_2O_3.

Figure 6 studied the effect of the reaction time on the activity of the samples at a reaction temperature of 600 °C. The results show that the catalytic activity of the monometallic Ni/γ-Al_2O_3 catalyst begins to decrease after 30 minutes, the modification of the nickel catalyst with cobalt oxide increases its activity. The cat-

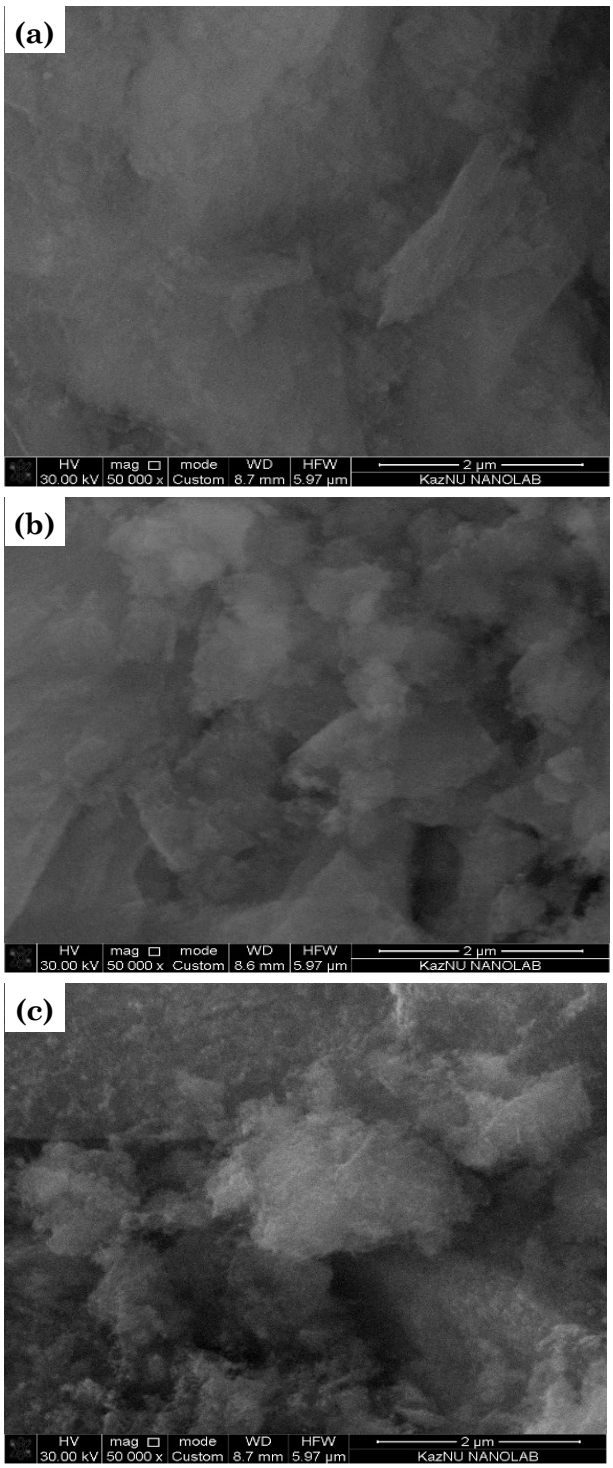

Figure 7. SEM micrographs of samples after testing them in methane decomposition for 300 min; (a) Ni/γ-Al_2O_3; (b) Co/γ-Al_2O_3; (c) Ni-Co/γ-Al_2O_3.

Copyright © 2021, ISSN 1978-2993

alytic activity of the bimetallic Ni-Co/γ-Al_2O_3 sample decreased after 60 minutes. The reason for the increase in the activity of the bimetallic catalyst may be associated with the formation of a nickel-cobalt alloy. It follows from these results that, in comparison with the monometallic catalysts Co/γ-Al_2O_3, Ni/γ-Al_2O_3, the bimetallic sample Ni-Co/γ-Al_2O_3 exhibits higher activity in the methane decomposition reaction. Monometallic Ni/γ-Al_2O_3 catalyst is more active than Co/γ-Al_2O_3. Cobalt oxide should not be considered as an active center for the decomposition of methane, but as a modifying additive to increase the activity of the nickel catalyst.

After testing in the decomposition of methane for 300 minutes, the catalysts were investigated by TGA and SEM methods. SEM results (Figure 7) confirm the presence of carbon in filamentary form. The results of the study of catalysts by the TGA method are shown in Figure 8. The thermochemical state of the sample is described by the curves: T (temperature), DTA (differential thermo analytical), TG (thermogravimetric) and DTG (differential thermogravimetric), the last curve is a derivative of the TG-function. As a result of dynamic heating of the samples, the DTA, DTG, and TG curves indicated manifestations caused by the occurrence of various types of reactions in the system. Among them carbon oxidation reactions, and polymorphic transformations of Ni and Co in the composition of the samples were determined.

Studies of the Ni/γ-Al_2O_3 sample under dynamic heating conditions (from 20 to 1000 °C) showed on the thermal curves a series of effects due to the emission into the atmosphere of molecular water (5.75%), carbon (C = 4.0%) and loosely bound solid particles from the product of the final calcination during its sublimation. All these emissions were within the range of 20–160 °C, 255–576 °C, and 576–1000 °C, respectively, Figure 8. Due to the small amount of these thermally active components in the sample, the DTA line reacted weakly to the endothermic effects of dehydration, leaving only weakly developed peaks on the curve at 105 and 190 °C. Carbon oxidation in the range 255–576 °C also proceeded without any special exothermic deviations of the curve under consideration. It should be noted that this DTA curve has a pronounced endothermic effect at 450 °C, which indicates a polymorphic transformation of the metal component, Ni, present in the complex.

The thermal behavior of Co/γ-Al_2O_3 (Figure 9) over the entire measured temperature range is similar to that of the Ni/γ-Al_2O_3 sample (Figure 8). However, in contrast to it, the considered cobalt complex includes a smaller number of centers holding H_2O, OH, and C. In this regard, the total weight loss (9.26%) of the system under consideration was lower than the weight loss (17%), which is marked by the Ni/γ-Al_2O_3 sample. The studied system also left on the DTA-curve an endothermic manifestation at 450 °C, which is associated with a reversible polymorphic transition of the cobalt-containing component of the sample from the α to β state

The heating curves of Ni-Co/γ-Al_2O_3 differ significantly from the curves of the above catalysts. The main difference when the sample is

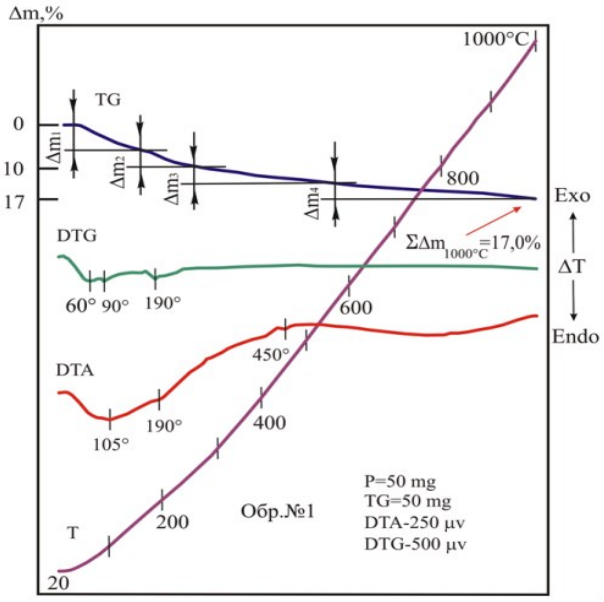

Figure 8. Derivatogram of Ni/γ-Al_2O_3 sample.

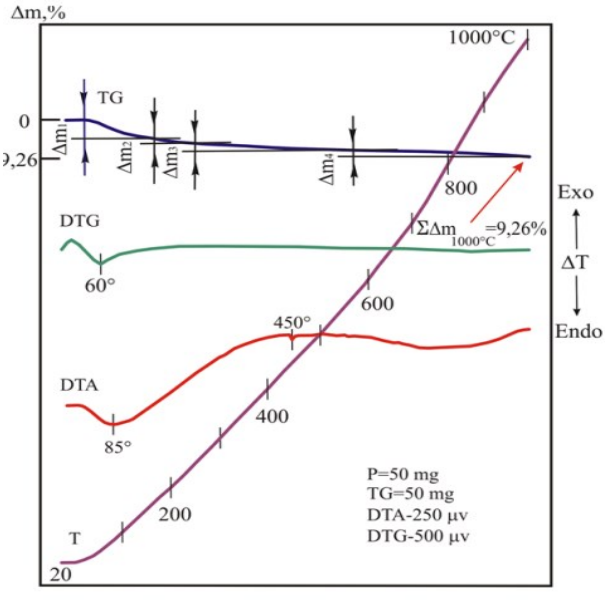

Figure 9. Derivatogram of Co/γ-Al_2O_3 sample.

Copyright © 2021, ISSN 1978-2993

heated in the range of 240–570 °C is the introduction of a large flow of thermal energy into the system, caused by combustion in the carbon sample. The observed heat flux formed a powerful exothermic effect on the DTA curve with a peak at 335 °C. The sample weight is reduced by 11.26% (a well-defined step on the thermogravimetric curve). The combustion rate of carbon (over time and temperature) is well controlled by the downward descending peak marked on the DTG curve, 335 °C in Figure 10.

4. Conclusion

The study of the activity of low-percentage monometallic and bimetallic nickel, cobalt-containing catalysts in the decomposition of methane in the temperature range 550–800 °C showed that, in comparison with monometallic catalysts Co/γ-Al_2O_3, Ni/γ-Al_2O_3, the bimetallic of Ni-Co/γ-Al_2O_3 exhibits more high activity in the reaction of methane decomposition. According to their activity in the conversion of methane at 600 °C, the catalysts can be arranged in the following order: Ni-Co/γ-Al_2O_3 (X_{CH_4} = 86%) > Ni/γ-Al_2O_3 (X_{CH_4} = 15.3%) > Co/γ-Al_2O_3 (X_{CH_4} = 1.2%). It was determined that cobalt oxide should not be considered as an active center for the decomposition of methane, but as a modifying additive to increase the activity of the nickel catalyst.

The study of the physicochemical characteristics of the catalysts by BET, XRD, SEM, TPR-H_2, and TGA showed that the modification of Ni/γ-Al_2O_3 with cobalt oxide leads to a uniform distribution of nanosized particles of the active phase on the surface of the support granules in the form of a homogeneous dispersion. An increase in the activity of a bimetallic catalyst in the decomposition of methane in comparison with monometallic catalysts is due to an increase in the dispersion of the active phases of the catalyst, as well as the formation of a nickel-cobalt alloy. In this case, the reducibility of the catalyst is facilitated, which ensures an increase in the concentration of metal particles - active centers, which can be the reason for the increase in the catalytic properties of the bimetallic catalyst.

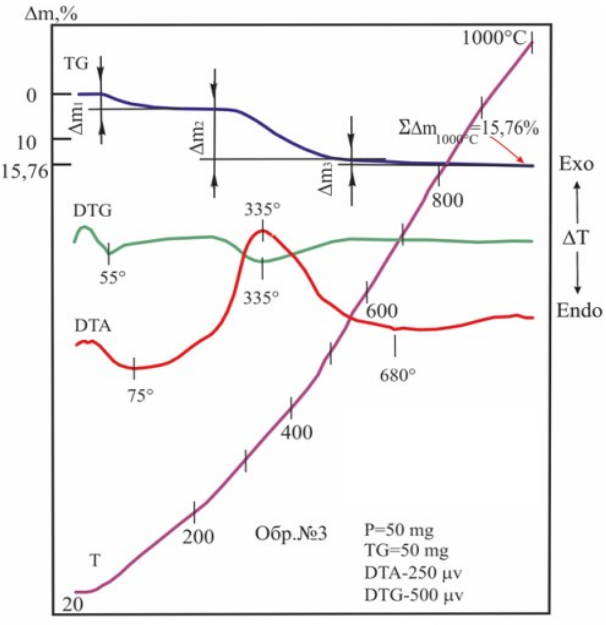

Figure 10. Derivatogram of Ni-Co/γ-Al_2O_3 sample.

Acknowledgements

This research is funded by the Science Committee of the Ministry of Education and Science of the Republic of Kazakhstan (Grant № AP08855564).

References

[1] http://atomicexpert.com/hydrogen_energy (Accessed on March 03, 2018)

[2] Soloviev, S.O. (2012). Oxidative Reforming of Methane on Structured Ni–Al_2O_3/Cordierite Catalysts. *Catalysis in Industry,* 4, 1–10. DOI: 10.1134/S2070050412010114.

[3] Soloviev, S.O., Gubareni. I.V., Orlyk, S.M. (2018). Oxidative Reforming of Methane on Structured Nickel–Alumina Catalysts: a Review. *Theoretical and Experimental Chemistry,* 54, 293–315. DOI: 10.1007/s11237-018-9575-5.

[4] Karaismailoglu, M., Figen, H.E., Baykara, S.Z. (2019). Hydrogen production by catalytic methane decomposition over yttria doped nickel based catalysts. *International Journal Hydrogen Energy*, 44, 9922–9929. DOI: 10.1016/j.ijhydene.2018.12.214.

[5] Rastegarpanah, A., Rezaei, M., Meshkani, F., Zhang, K., Zhao, X., Pei, W., Liu, Y., Deng, J., Arandiyan, H., Dai, H. (2019). Influence of group VIB metals on activity of the Ni/MgO catalysts for methane decomposition. *Applied Catalysis B,* 248, 515–525. DOI: 10.1016/j.apcatb.2019.01.067.

[6] De Roseno, K.T., Schmal, M., Brackmann, R.M., Alves, R.G. (2019). Partial oxidation of methane on neodymium and lanthanium chromate based perovskites for hydrogen production. *International Journal Hydrogen Energy*, 44, 8166–8177. DOI: 10.1016/j.ijhydene.2019.02.039.

Copyright © 2021, ISSN 1978-2993

[7] Dossumov, K., Ergazieva, G.E., Ermagambet. B.T., Telbayeva, M.M., Mambetova, M.M., Myltykbayeva, L.K., Kassenova, Z.M. (2020). Role of ceria in several energy-related catalytic transformations. *Chemical Papers,* 74, 373–388. DOI: 10.1007/s11696-019-00921-8.

[8] Stiegel, G.J., Ramezan, M. (2006). Hydrogen from coal gasification: An economical pathway to a sustainable energy future. *International Journal Coal Geol,* 65, 173–190. DOI: 10.1016/j.coal.2005.05.002.

[9] Grigoriev, S.A., Porembsky, V.I., Fateev, V.N. (2006). Pure hydrogen production by PEM electrolysis for hydrogen energy. *International Journal Hydrogen Energy*, 31, 171–175. DOI: 10.1016/j.ijhydene.2005.04.038.

[10] Zeng, K., Zhang, D. (2010). Recent progress in alkaline water electrolysis for hydrogen production and applications1o. *Progress in Energy and Combustion Science,* 36, 307–326. DOI: 10.1016/j.pecs.2009.11.002.

[11] Shahzad, K., Tahir, M.B., Sagir, M. (2019). Engineering the performance of heterogeneous WO_3/fullerene@Ni_3B/$Ni(OH)_2$ Photocatalysts for Hydrogen Generation. *International Journal Hydrogen Energy,* 44, 21738–21745. DOI: 10.1016/j.ijhydene.2019.06.148

[12] Tahir, M.B., Riaz, K.N., Asiri, A.M. (2019). Boosting the performance of visible light-driven WO_3/g-C_3N_4 anchored with $BiVO_4$ nanoparticles for photocatalytic hydrogen evolution. *International Journal Energy Research,* 43, 5747–5758. DOI: 10.1002/er.4673.

[13] Shabani, S., Delavar, M.A., Azmi, M. (2013). Investigation of biomass gasification hydrogen and electricity co-production with carbon dioxide capture and storage. *International Journal Hydrogen Energy,* 38, 3630–3639. DOI: 10.1016/j.ijhydene.2013.01.066.

[14] Holmen, A. (2209). Direct conversion of methane to fuels and chemicals. *Catalysis Today*, 142(1–2), 2–8. DOI: 10.1016/j.cattod.2009.01.004.

[15] Dossumov, K., Ergazieva, G.E., Ermagambet, B.T., Myltykbaeva, L.K., Telbaeva, M.M., Mironenko, A.V., Mambetova, M.M., Kasenova, G. (2020). Morphology and Catalytic Properties of Cobalt-Containing Catalysts Synthesized by Different Means. *Russian Journal Physic Chemistry A,* 94, 880–882. DOI: 10.1134/S0036024420040020.

[16] Dossumov, K., Yergazyieva, G.Y., Myltykbayeva, L.K., Suyunbayev, U., Asanov, N.A., Gyulmaliev, A.M. (2015). Oxidation of Methane over Polyoxide Catalysts. *Coke Chemistry*, 58(5), 178–183. DOI: 10.3103/S1068364X15050026.

[17] Mondal, K.C., Chandran, S.R. (2014). Evaluation of the economic impact of hydrogen production by methane decomposition with steam reforming of methane process. *International Journal Hydrogen Energy,* 39, 9670–9674. DOI: 10.1016/j.ijhydene.2014.04.087

[18] Keipi, T., Tolvanen, H., Konttinen, J. (2018). Economic analysis of hydrogen production by methane thermal decomposition: Comparison to competing technologies. *Energy Convers Manage*, 159, 264–273. DOI: 10.1016/j.enconman.2017.12.063.

[19] Chen, J., Ou, Z., Chen, H., Song, S., Wang, K., Wang, Y. (2021). Recent developments of nanocarbon based supports for PEMFCs electrocatalysts. *Chinese Journal of Catalysis,* 42(8), 1297–1326. DOI: 10.1016/S1872-2067(20)63736-6.

[20] Hazzim, F., Abbas, U.P., Ashik, S.A., Mohammed, W.M., Ashri, W.D. (2021). Impact of reactor materials on methane decomposition for hydrogen production. *Chemical Engineering Research and Design,* 174, 127–136. DOI: 10.1016/j.cherd.2021.08.005.

[21] Tahir, M.B., Nabi, G., Khalid, N.R., Rafique, M. (2018). Role of europium on WO3performance under visible-lightfor photocatalytic activity. *Ceramics International*, 44, 5705–5709. DOI: 10.1016/j.ceramint.2017.12.223.

[22] Khalid, N.R., Liaqat, M., Tahir, M.B., Nabi, G., Iqbal, T., Niaz, N.A. (2018). The role of graphene and europium on TiO_2 performance for photocatalytic hydrogen evolution. *Ceramics International,* 44, 546. DOI: 10.1016/j.ceramint.2017.09.209.

[23] Maeda, K., Domen, K. (2010). Photocatalytic Water Splitting: Recent Progress and Future Challenges. *Journal Physical Chemistry Letters,* 1, 2655–2661. DOI: 10.1021/jz1007966.

[24] Qian, J.X., Chen, T.W., Enakonda L.R., Liu, D.B., Mignani, G., Basset, J.M., Zhou, L. (2020). Methane decomposition to produce COx-free hydrogen and nano-carbon over metal catalysts: A review. *International Journal of Hydrogen Energy,* 45, 7981–8001. DOI: 10.1016/j.ijhydene.2020.01.052.

[25] Karimi, S., Bibak, F., Meshkani, F., Rastegarpanah, A., Deng, J., Liu, Y., Dai, H. (2021). Promotional roles of second metals in catalyzing methane decomposition over the Ni-based catalysts for hydrogen production: A critical review. *International Journal Hydrogen Energy*, 46, 20435–20480. DOI: 10.1016/j.ijhydene.2021.03.160.

Copyright © 2021, ISSN 1978-2993

[26] Torres, D., Pinilla, J.L., Suelves, I. (2020). Cobalt doping of a-Fe/Al_2O_3 catalysts for the production of hydrogen and high-quality carbon nanotubes by thermal decomposition of methane. *International Journal Hydrogen Energy,* 45(38), 19313–19323. DOI: 10.1016/j.ijhydene.2020.05.104.

[27] Silva, R.R., Oliveira, H.A., Guarino, A.C., Toledo, B.B., Moura, M.B., Oliveira, B.T., Passos, F.B. (2016). Effect of support on methane decomposition for hydrogen production over cobalt catalysts. *International Journal Hydrogen Energy,* 41(16), 6763–6772. DOI: 10.1016/j.ijhydene.2016.02.101.

[28] Fan, Z., Weng, W., Zhou, J., Gu, D., Xiao, W. (2021). Catalytic decomposition of methane to produce hydrogen: A review. *Journal Energy Chemistry,* 58, 415–430. DOI: 10.1016/j.jechem.2020.10.049.

[29] Liu, F., Xuan, G., Ai, L., Liu, Q., Yang, Li. (2021). Key factors that affect catalytic activity of activated carbon-based catalyst in chemical looping methane decomposition for H_2 production. *Fuel Process Technol,* 215, 106745. DOI: 10.1016/j.fuproc.2021.106745.

[30] Wang, J., Yang, Z., Yang, K., Peng, S. (2021). Kinetics of oxygen reaction in porous $La_{0.6}Sr_{0.4}Co_{0.2}Fe_{0.8}O_{3-\delta}$-$Ce_{0.8}Gd_{0.2}O_{1.9}$ composite electrodes for solid oxide cells. *International Journal Hydrogen Energy,* 46(50), 25608–25619. DOI: 10.1016/j.ijhydene.2021.05.071.

[31] Muhammad, A.F.S., Ali, A., Saidur, R., Masiran, N., Salam, A., Abdullah, B. (2018). Recent advances in cleaner hydrogen productions via thermo-catalytic decomposition of methane: Admixture with hydrocarbon. *International Journal Hydrogen Energy,* 43, 18713–18734. DOI: 10.1016/j.ijhydene.2018.08.091.

[32] Makvandi, S., Alavi, S.M. (2011). COx Free Hydrogen Production by Catalytic Decomposition of Methane Over Porous Ni/Al_2O_3 Catalysts. *Iranian Journal of Chemical Engineering,* 8(4), 24–33.

[33] Chai, S.P., Seah, C.M., Mohamed, A.R. (2011). A parametric study of methane decomposition into carbon nanotubes over 8Co-2Mo/Al_2O_3 catalyst. *Journal of Natural Gas Chemistry,* 20, 84–89. DOI: 10.1016/S1003-9953(10)60151-X.

[34] Yergaziyeva, G.Y., Dossumov, K., Mambetova, M.M., Strizhak, P.Y., Kurokawa, H., Baizhomartov, B. (2021). Effect of Ni, La, and Ce Oxides on a Cu/Al_2O_3 Catalyst with Low Copper Loading for Ethanol Non-oxidative Dehydrogenation**.** *Chemical Engineering and Technology*, 44(10), 1890–1899. DOI: 10.1002/ceat.202100112.

[35] Dosumov, K., Ergazieva, G.E., Churina, D.Kh., Tel'Baeva, M.M. (2014). Cerium-containing catalysts for converting ethanol into ethylene. *Russian Journal of Physical Chemistry A*, 88(10), 1806–1808. DOI: 10.1134/S0036024414100094.

[36] Ergazieva, G.E., Telbayeva, M.M., Popova, A.N., Ismagilov, Z.R., Dossumov, K., Myltykbayeva, L.K., Dodonov, V.G., Sozinov, S.A., Niyazbayeva, A.I. (2021). Effect of preparation method on the activity of bimetallic Ni-Co/Al_2O_3 catalysts for dry reforming of methane. *Chemical Papers,* 75, 2765–2774. DOI: 10.1007/s11696-021-01516-y.

[37] Wan, C., Shi, Z., Huang, M., Pan, J., Luo, R., Li, D., Jiang, L. (2020). Influence of alloying on the catalytic performance of NieAl catalyst prepared from hydrotalcite-like compounds for methane decomposition. *International Journal Hydrogen Energy,* 46(5), 3833–3846. DOI: 10.1016/j.ijhydene.2020.10.186.

[38] Dossumov, K., Yergazieva, G.Y., Myltykbaieva, L.K., Asanov, N.A.(2016). Effect of Co, Ce, and La oxides as modifying additives on the activity of an NiO/-Al_2O_3 Catalyst in the oxidation of methane to give Synthesis Gas. *Theoretical and Experimental Chemistry,* 52, 119–122. DOI: 10.1007/s11237-016-9459-5.

[39] Lisboa, J.S., Terra, L.E., Silva, P.R., Saitovitch, H., Passos, F.B. (2011). Investigation of Ni/Ce–ZrO_2 catalysts in the autothermal reforming of methane. *Fuel Process Technology,* 92:2075–2082. DOI: 10.1016/j.fuproc.2011.06.011.

[40] Montoya, J.A., Romero-Pascual, E., Gimon, C., Del Angel, P., Monzón, A. (2000). Methane reforming with CO_2 over Ni/ZrO_2–CeO_2 catalysts prepared by sol–gel. *Catalysis Today,* 63, 71–85. DOI: 10.1016/S0920-5861(00)00447-8.

[41] Xu, J.K., Zhou, W., Li, Z.J., Wang, J.H., Ma, J.X. (2009). Biogas reforming for hydrogen production over nickel and cobalt bimetallic catalysts. *International Journal Hydrogen Energy,* 34, 6646–6654. DOI: 10.1016/j.ijhydene.2009.06.038.

[42] Reynoso, A.J., Ayastuy, J.L., Iriarte-Velasco, U., Gutiérrez-Ortiz, M.A. (2018). Cobalt aluminate spinel-derived catalysts for glycerol aqueous phase reforming. *Applied Catalysis B,* 239, 86–101. DOI: 10.1016/j.apcatb.2018.08.001.

Copyright © 2021, ISSN 1978-2993

[43] Karabanov, A.V., Shmanovskaya, A.L., Kutovoy, A.A., Aleksenko, K.N., Vasilenko, A.A., Ivanenko, S.S., Yagmurov, V.Y., Larina, M.V. (2019). Effect of alumina modification on a cobalt Fischer-Tropsch catalyst promoted with manganese oxide. *Engineering Bulletin of the Don,* 1, 25–29. URL: ivdon.ru/ru/magazine/archive/n1y2019/5523 (in Russian).

[44] Ay, H., Üner, D. (2015). Dry reforming of methane over CeO_2 supported Ni, Co and Ni-Co catalysts. *Applied Catalysis B,* 179, 128–138. DOI: 10.1016/j.apcatb.2015.05.013.

[45] Klissurski, D.G., Uzunova, E.L. (1991). Synthesis of Nickel Cobaltite Spinel from Co-precipitated Nickel-Cobalt Hydroxide Carbonate. *Chemical Materials,* 3, 1060–1063. DOI: 10.1021/cm00018a021.

[46] Fang, A., Zhejiang, J. (2020). $NiCo_2O_4$ nanoparticles: an efficient and magnetic catalyst for Knoevenagel condensation. *University-Science A (Applied Physics & Engineering),* 21(1), 74–84. DOI: 10.1631/jzus.A1900535.

[47] Ashokkumar, S., Ganesan, V., Ramaswamy, K.K., Balasubramanian, V. (2018). Bimetallic Co–Ni/TiO_2 catalysts for selective hydrogenation of cinnamaldehyde. *Research on Chemical Intermediates,* 44, 6703–6720. DOI: 10.1007/s11164-018-3517-7.

[48] Li, L., Lu, P., Yao, Y., Ji, W. (2021). Silica-encapsulated bimetallic Co–Ni nanoparticles as novel catalysts for partial oxidation of methane to syngas. *Catalysis Communications,* 26, 72–77. DOI: 10.1016/j.catcom.2012.05.005.

[49] Tezel, E., Figen, H.E., Baykara, S.Z. (2019). Hydrogen production by methane decomposition using bimetallic NieFe catalysts. *International Journal Hydrogen Energy,* 44(20), 9930–9940. DOI: 10.1016/j.ijhydene.2018.12.151.

Copyright © 2021, ISSN 1978-2993